



Snow depth product over Antarctic sea ice from 2002 to 2020 using multisource passive microwave radiometers

Xiaoyi Shen^{1,2}, Chang-Qing Ke^{1,2}, Haili Li^{1,2}

¹ School of Geography and Ocean Science, Nanjing University, Nanjing, 210023, China

5 ² Jiangsu Provincial Key Laboratory of Geographic Information Science and Technology, Nanjing University, Nanjing, 210023, China

Correspondence to: Chang-Qing Ke (kecq@nju.edu.cn)

Abstract. Snow over sea ice controls energy budgets and affects sea ice growth/melting, and thus has essential effects on the climate. Passive microwave radiometers can be used for basin-scale snow depth estimation at a daily scale; however, previously published methods applied to Antarctica clearly underestimated snow depth, limiting their further application. Here, we estimated snow depth using microwave radiometers and a newly constructed, robust method by incorporating lower frequencies, which have been available from AMSR-E and AMSR-2 since 2002. A regression analysis using 7 years of Operation IceBridge (OIB) airborne snow depth measurements showed that the gradient ratio (GR) calculated using brightness temperatures in vertically polarized 37 and 19 GHz, i.e., GR(37/7), was optimal for deriving Antarctic snow depth, with a correlation coefficient of -0.64. We hence derive new coefficients based on GR(37/7) to improve the current snow depth estimation from passive microwave radiometers. Comparing the new retrieval with in situ measurements from the Australian Antarctic Data Centre showed that this method outperformed the previously available method, with a mean difference of 5.64 cm and an RMSD of 13.79 cm, compared to values of -14.47 cm and 19.49 cm, respectively. A comparison to shipborne observations from Antarctic Sea Ice Processes and Climate indicated that in thin ice regions, the proposed method performed slightly better than the previous method (with RMSDs of 16.85 cm and 17.61 cm, respectively). Comparable performances during the growth and melting seasons suggest that the proposed method can still be used during the melting season. Gaussian error propagation found an average snow depth uncertainty of 3.81 cm, which accounted for 12% of the estimated mean snow depth. We generated a complete snow depth product over Antarctic sea ice from 2002 to 2020 on a daily scale, and negative trends could be found in all sea sectors and seasons. This dataset (including both snow depth and snow depth uncertainty) can be downloaded from National Tibetan Plateau Data Center, Institute of Tibetan Plateau Research, Chinese Academy of Sciences at <http://data.tpdc.ac.cn/en/disallow/61ea8177-7177-4507-aeeb-0c7b653d6fc3/> (Shen and Ke, 2021, DOI: 10.11888/Snow.tpdc.271653).

1 Introduction

Snow is a basic element in the Antarctic sea ice system and it changes the surface albedo of sea ice (Petrich et al., 2012), controls energy exchanges between the atmosphere and ocean (Kwok & Untersteiner, 2011) and affects sea ice growth and



melting (Maykut et al., 1971, Sturm et al., 2002). Thus, it has essential climatic effects (Webster et al., 2018). Because snow depth is a fundamental property of snow cover, knowing how it changes is crucially important for understanding rapid changes in the Antarctic climate. Snow depth is also an essential input for sea ice thickness estimation (Kwok et al., 2020, Giles et al., 2008), and its accuracy will greatly affect the reliability of sea ice thickness estimates. Hence, from the perspectives of climate and sea ice thickness estimation, basin-scale snow depth products in Antarctica, especially over long times, are urgently needed.

Although in situ measurements of snow depth over Antarctic sea ice have very high accuracy and precision, their spatial and temporal coverage are quite limited. Airborne snow depth measurements can cover regions of thousands of square kilometres, but they are cost intensive and represent only limited regions. Only satellites can obtain snow depth at the hemispheric scale, and individual and multisource satellites have been applied for snow depth estimation, e.g., passive microwave radiometers (Markus and Cavalieri, 1998, Comiso et al., 2003, Maaß et al., 2013), satellite laser altimeters (Kern et al., 2016), and a combination of satellite radar and laser altimeters (Kwok et al., 2019). Given both the basin-scale coverage and the temporal resolution requirements, passive microwave radiometers are the best tools to derive a long data record of snow depth in Antarctica with daily coverage.

The theoretical basis of snow depth estimation from microwave radiometers is that the volume scattering of upwelling snow cover affects the radiation signal emitted from the underlying sea ice and reduces the observed brightness temperatures (Markus and Cavalieri, 1998). Thus, the observed brightness temperatures are related to the observation frequency and snow depth, and the snow brightness temperature increases as snow depth decreases or observation frequency increases. Based on this principle, Markus et al. (1998) used correlation analysis for the measured snow depth and brightness temperatures observed from the Special Sensor Microwave/Imager (SSM/I) in Antarctica. They found that the gradient ratio (GR) calculated from vertical polarized brightness temperatures at 19 GHz and 37 GHz had the highest correlation with measured snow thickness with a correlation coefficient of -0.60. An empirical linear regression equation was then derived for snow depth estimation, and the regression coefficients were updated for successor microwave radiometers (i.e., Advanced Microwave Scanning Radiometer for EOS (AMSR-E), Comiso et al., 2003).

Although this method can derive basin-scale snow depth, due to the snow penetration depth when 37 and 19 GHz frequencies (i.e., higher frequencies) are used and the strong influence liquid water in the snow layer has on the observed radiation from microwave radiometers, this method is limited to dry snow less than 50 cm thick, which is clearly less than the snow cover over Antarctic sea ice (Kwok et al., 2014). Given these influences, this method obviously underestimates thickness by a factor of 2.3 (Worby et al., 2008a) or between 2 and 4 (Kern et al., 2016). Since 2002, successful launches of AMSR-E and successor Advanced Microwave Scanning Radiometer 2 (AMSR-2) have provided a chance to estimate snow depth with lower frequencies. Lower frequencies are sensitive to deeper ice layers, are less affected by liquid water in the snow layer and weather conditions (Rostosky et al., 2018) and have been used to improve snow depth estimation over Arctic sea ice (Rostosky et al., 2018, Kilic et al., 2019, Winstrup et al., 2019, Braakmann-Folgmann et al., 2019). Compared to the Arctic, snow depth over Antarctic sea ice is usually thicker (Kern et al., 2016), more heterogeneous (Massom et al., 2001)



65 and less affected by surface melting; hence, lower frequencies tend to be more reliable for estimating snow depth. However, these methods have not been tested or applied to Antarctic snow depth estimation until now.

In the present study, we attempt to construct a new and effective method to estimate snow depth over Antarctic sea ice. For the potential improvement of snow depth estimation using low-frequency signals, AMSR-E and AMSR-2 were used to derive new regression coefficients in the estimation equation. A detailed introduction to these data is shown in Section 2. Section 3 describes the methods for snow depth and uncertainty estimations, and the accuracy evaluation is shown in Section 4. Section 5 shows the spatiotemporal variation in the derived Antarctic snow depth between 2002 and 2020. Section 6 discusses the uncertainty sources of the proposed method, Section 7 gives the data availability and Section 8 concludes this paper.

2 Data

75 2.1 AMSR-E, AMSR-2 and SSMIS brightness temperature observations

To generate a complete time series of snow depth data over Antarctic sea ice, multiple passive microwave radiometers were used, including AMSR-E, AMSR-2 and the Special Sensor Microwave Imager Sounder (SSMIS). Between June 2002 and September 2011, AMSR-E data were used. With an observation angle of 55° , AMSR-E can provide daily brightness temperature observations in the Arctic and in Antarctica. Six frequency channels were applied, i.e., 6.93, 10.7, 18.7, 23.8, 80 36.5 and 89.0 GHz, and each channel had both horizontal and vertical polarizations. Here, the AMSR-E/Aqua Daily L3 25 km Brightness Temperature and Sea Ice Concentration Polar Grids (Version 3) product from the National Snow and Ice Center (NSIDC) were used, and pre-processing, bias correction and quality control were all applied.

Between 1 June 2012 and May 2020, AMSR-2 data were used. Compared to AMSR-E, AMSR-2 has the same observation angle and frequency channels but has an additional frequency at 7.3 GHz. Here, the NSIDC AMSR-E/AMSR-2 Unified L3 85 Daily 25 km Brightness Temperature and Sea Ice Concentration Polar Grids (Version 1) product was used, and pre-processing, bias correction and quality control were also applied.

Brightness temperature observations from SSMIS were used to fill the gap in AMSR-E and AMSR-2 data between October 2011 and May 2012. The DMSP SSM/I-SSMIS Daily Polar Gridded Brightness Temperature (Version 4) product was used here because it has the same spatial and temporal resolutions as the two brightness temperature products mentioned 90 above. However, SSMIS does not have lower frequency channels (lower than or equal to 19 GHz) than AMSR-E and AMSR-2; hence, the corresponding snow depth estimation equation was adjusted accordingly, as shown in Section 3.

To generate consistent brightness temperature observations from 2002 to 2020, a consistency correction should be applied in the three microwave radiometer datasets. The SSMIS brightness temperature observations were calibrated based on the AMSR-E data, and we calibrated the AMSR-2 data to AMSR-E based on the correction parameters from Du et al. (2014). 95 These brightness temperature observations were also used to obtain sea ice concentrations by using the ARTIST Sea Ice (ASI) algorithm (Spreen et al., 2008).



2.2 Operational IceBridge airborne snow depth measurements

The initial aim of the Operational IceBridge (OIB) airborne mission is to fill the observation gap between ICESat and ICESat-2. This mission provides annual measurements of snow depth over sea ice, elevation and thickness of sea ice, and information on sea ice types in the Arctic and Antarctica. Due to the large coverage of measurements, it was suitable to evaluate satellite-derived parameters. In the OIB airborne mission, Airborne Topographic Mapper (ATM), a laser altimeter, is used to measure the elevation of the sea ice surface. Its footprint depends on the observation angle of the pulsed laser and flight altitude. The size is approximately 1 m (Kurtz et al., 2013, Schenk et al., 1999), and the location and elevation measurements accuracies for individual measurements are approximately 1 m and 0.1 m (or better, Krabill et al., 1995), with a vertical precision of 3 cm (Martin et al., 2012).

The measured elevations were used to derive the total freeboard. Following Zwally et al. (2008) and Kern et al. (2015), the lowest 2% elevations in a 50 km segment along the track were regarded as the sea surface heights, and the mean value was calculated as the mean sea surface segment height (MSSH). Other points were taken as sea ice measurement points, and the corresponding total freeboard was calculated by misusing the local MSSH from the sea ice surface heights.

Radar is used to measure the snow depth in the OIB airborne mission. However, for snow cover over Antarctic sea ice, the snow-ice interface is hard to distinguish (Willatt et al., 2009, Giles et al., 2008) due to the complicated snow morphology often found in Antarctica (Massom et al., 2001). Accurate snow depth detection needs more in situ investigations and in-depth studies. Considering these influences, snow depth was derived from the total freeboard as described in Ozsoy-Cicek et al. (2013). The corresponding linear equations were constructed in six individual sea sectors in the Southern Ocean, with correlation coefficients ranging from 0.81 to 0.99. These have been widely used in previously published studies to obtain Antarctic sea ice parameters (Xie et al., 2013, Kern et al., 2016, Li et al., 2018).

OIB ATM data collected in 2009, 2010, 2012–2014, and 2016–2018 were used, and no data could be obtained for the missing years. The OIB ATM spatial distribution data used are shown in Fig. 1a. Most of the OIB ATM data came from western Antarctica and one track covered the Ross Sea sector. These measurements covered both the thicker snow in the Weddell Sea sector and the thinner snow in the Ross Sea sector and provided comprehensive measurements for the development of satellite-based snow depth estimation methods.

2.3 AADC in situ measurement data

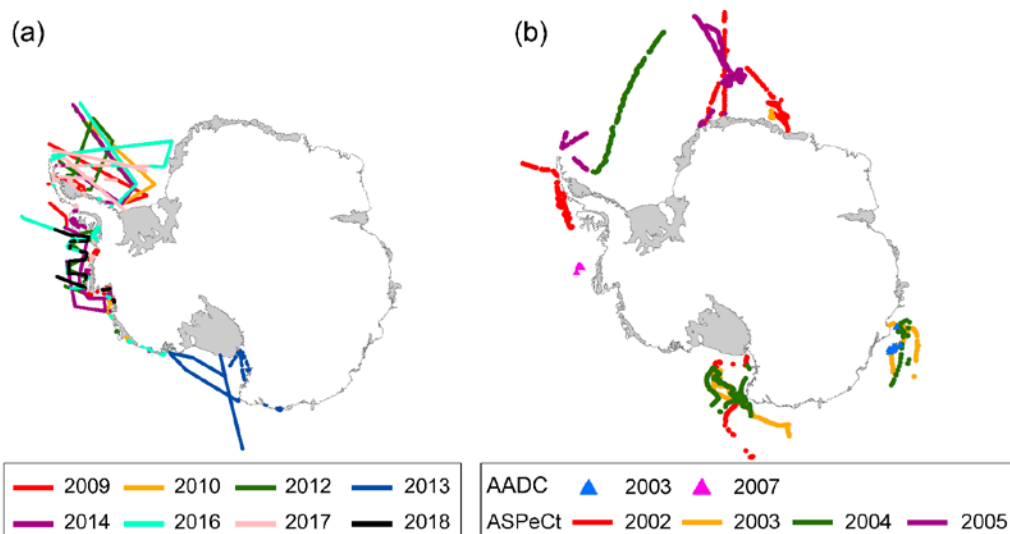
We used in situ snow depth measurements from the Australian Antarctic Data Centre (AADC) to evaluate the proposed method. AADC in situ data include measurements of sea ice and snow from 1985 to 2007. This dataset provides records of snow depth, sea ice freeboard and sea ice thickness. Here, AADC data from 2003 and 2007 were used to compare our snow depth estimation results, which were mainly located in eastern and western Antarctica (Fig. 1b). Although in situ measurements are relatively rare, AADC has measurements of both thick and thin ice, which provide a comprehensive and accurate evaluation of estimated snow depth.



2.4 ASPeCt shipborne observation data

130 We also used snow depth observations from the Antarctic Sea Ice Processes and Climate (ASPeCt) mission to evaluate the
estimated snow depth. These data (including observations of snow depth, sea ice thickness and ice type) were obtained every
hour within a 1 km radius of the ship. We followed the Worby et al. (2008b) method to reduce the sampling bias caused by
temporal data collection and variable ship speed by removing observations within 6 nautical miles of previous observations.
This method ensured the independence of each record. As the microwave radiometer observes both undeformed and
135 deformed sea ice, the ‘averaged snow depth’ record was used to compare to the microwave radiometer-derived snow depth.
This record considers the undeformed thickness, ridge height, and ridge coverage, which are the overall estimates of
observed snow depths. According to the error analysis in Worby et al. (2008b), $\pm 20\%$ bias of ASPeCt data is found for
undeformed ice thicker than 0.3 m, and $\pm 30\%$ bias is found for deformed ice.

This dataset contains snow depth measurements from 81 cruises between 1981 and 2005. Here, we used ASPeCt data
140 from individual months (except for February, May, June and July) between 2002 and 2005, which covered various types of
sea ice and most sea sectors in the Southern Ocean (Fig. 1b).



145 **Figure 1.** The spatial-temporal distributions of OIB airborne measurements (a), ASPeCt shipborne observations and AADC
in situ measurements (b).



3 Method

3.1 The selection of optimal frequency channels

Although lower frequencies tend to better estimate snow depth, we used all frequencies to find the optimal frequency channels. All available combinations were compared to the OIB airborne snow depth measurements, and only VV combinations were used, since they had better performance than the HH combinations (Rostovsky et al., 2018). To reduce the effect of uneven OIB measurement distributions within the microwave radiometer grid cells caused by their resolution difference, on the same day, one microwave radiometer grid cell (i.e., 25 km × 25 km) should contain at least 2500 OIB measurement points. Since Antarctic OIB airborne missions are launched in October or November each year, air temperatures could be higher than the melting point and cause surface melting. To reduce the influence of the snow layer's liquid water on brightness temperatures observed by microwave radiometers, we excluded brightness temperatures that were assumed to be affected by liquid water based on the 2 m air temperature (T2m) data from ERA5 reanalysis data. If the T2m in a single grid cell during one day or during at least 5 of the 10 preceding days, is higher than 0 °C, the brightness temperatures were removed (Rostovsky et al., 2018).

Table 1 shows the correlation and root mean square deviation (RMSD) between OIB snow depth measurements and individual GRs. The combination of GR (37/19) and GR (19/10) was also applied here, since it was considered optimal for Arctic snow depth estimation (Markus et al., 2006). Different weightings had no obvious influence on the estimation result, and a weighting of 1:1 was used here.

Table 1. The relationships (including RMSD and correlation coefficient) between the OIB snow depth and different GRs.

GR	RMSD (cm)	Correlation coefficient	Number of grid cells
GR (37/24)	9.22	-0.61	
GR (37/19)	9.11	-0.62	
GR (37/11)	8.95	-0.64	
GR (37/7)	8.92	-0.64	
GR (24/19)	9.21	-0.61	
GR (24/11)	9.03	-0.63	
GR (24/7)	9.14	-0.62	740
GR (19/11)	9.15	-0.62	
GR (19/7)	9.46	-0.58	
GR (11/7)	10.62	-0.41	
<u>GR (37/19)+GR (19/10)</u>	8.96	-0.64	
2			



Except for GR (11/7), most GRs had good correlations with OIB snow depth, with correlation coefficients of >0.57 and RMSDs of <10 cm. GR (37/7), GR (37/11) and $\frac{GR(37/19)+GR(19/10)}{2}$ had better performances, and the root mean square residual and standard deviations of the derived regression coefficients were 80, 83 and 80 and 0.44, 0.57 and 0.50, respectively. GR (37/7) performed optimally across all evaluation indices; thus, in the following section, we used GR (37/7) to construct a new snow depth estimation equation.

3.2 The derivation of new snow depth estimation equation

Fig. 2a shows the scatter plot between the OIB snow depth and GR (37/7). To reduce the influence of outliers, only OIB snow depth data between the 5th to 95th percentiles were used to derive the equation coefficients. The corresponding regression equation can be derived as follows:

$$SD_{GR(37/7)}(\text{cm}) = 26.7 - 411 \cdot GR(37/7) \quad (1)$$

SSMIS frequencies were not as low as those of AMSR-E/2, meaning GR (37/7) could not be used with SSMIS data. Because of this, we used GR (37/19), which ranked next to GR (37/7), as shown in Table 1. The corresponding equation is listed as follows (Fig. 2b):

$$SD_{GR(37/19)}(\text{cm}) = 23.5 - 601 \cdot GR(37/19) \quad (2)$$

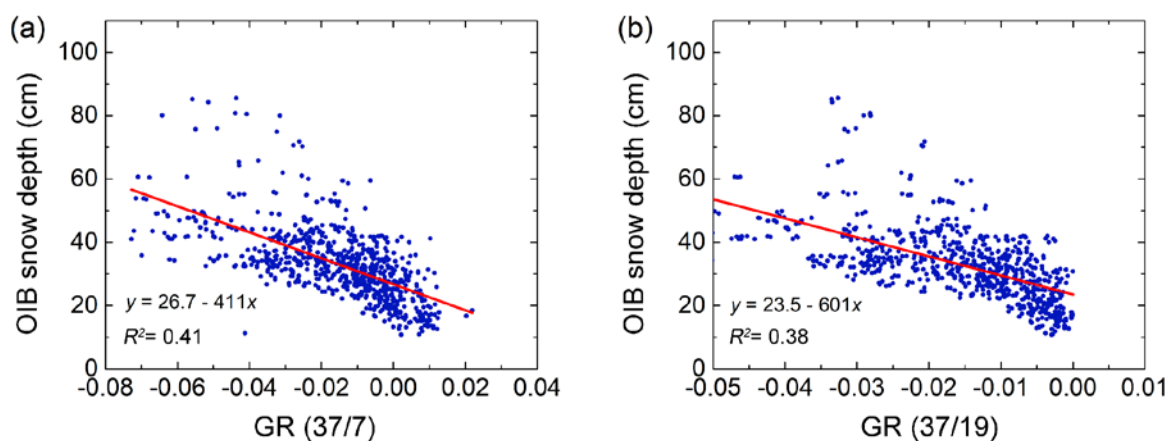


Figure 2. The scatter diagrams between the OIB snow depth and two GRs, i.e., GR (37/7) (a) and GR (37/19) (b).

To maintain the consistency of snow depth estimates based on two equations above, we compared their snow depth estimates during the OIB period. The snow depth estimations derived from the two equations agreed well and had an RMSD of 1.89 cm, and we corrected their original difference based on an empirical linear regression equation:



$$SD_{GR(37/7)}(\text{cm}) = SD_{GR(37/19)}(\text{cm}) - 0.03 \quad (3)$$

The snow depth from October 2011 to May 2012 was estimated based on Eq. (2) and Eq. (3).

190 3.3 The estimation of snow depth uncertainty

The snow depth uncertainty was estimated from the uncertainty of individual input variables using Gaussian error propagation. Brightness temperature and sea ice concentration uncertainties were assumed to be 0.5 K and 5% (Rostosky et al., 2018). Detailed calculation steps can be found in Rostosky et al. (2018).

Fig. 3 shows the spatial distributions of averaged snow depth uncertainty from 2002 to 2020 during four seasons: spring (October-December), summer (January-March), autumn (April-June) and winter (July-September) (Zwally et al., 2002). The snow depth uncertainty in summer (an average of 4.52 cm) was larger than that in other seasons due to the effect of liquid water in the snow layer. In autumn, winter and spring, the average snow depth uncertainties were approximately 3.66 cm, 3.33 cm and 3.74 cm, respectively. Spatially, smaller snow depth uncertainties were found in the sea ice interior, while larger uncertainties were found in the sea ice marginal region, which may be due to complex surface conditions there. The averaged snow depth uncertainties accounted for approximately 13%, 12%, 12% and 11% of the averaged snow depths in spring, summer, autumn and winter, respectively, and depended on the snow depth.

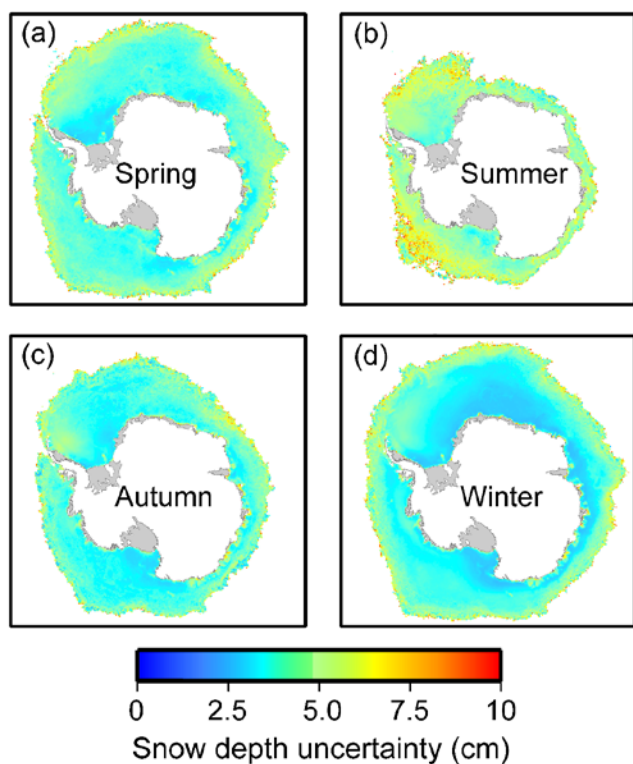


Figure 3. The spatial distributions of averaged snow depth uncertainty in different seasons from 2002 to 2020.



4 Accuracy evaluation

205 4.1 Self-evaluation of the proposed method

To prove the robustness of the proposed method, we calculated 7 pairs of regression coefficients (for Eq. (1)) based on each 6-year combination of OIB snow depth data between 2009 and 2018 (Table 2). Only regression coefficients calculated from more than 80 matched points were used for sensitivity analysis to ensure reliability. The uncertainty of the individual coefficient was estimated as its standard deviation. The estimated slope ranged from -474 to -349 with an uncertainty of 210 42.85, which caused a bias of <1 cm for the snow depth estimation; furthermore, the intercept varied from 25.4 to 28.3 with an uncertainty of 1.14. No obvious interannual variations could be found for either the slope or the intercept values.

Table 2. The regression coefficients of snow depth estimation equations based on OIB snow depth data in different years.

Excluded year	Intercept	Slope	Number of grid cells
2009	25.4	-417	161
2010	27.2	-445	88
2012	28.3	-349	147
2013	23.8	-707	40
2014	25.4	-394	103
2016	27.3	-474	134
2017	33.8	-176	68
All data	26.7	-411	740

215 Here, the OIB snow depth data in 2016 were used to self-evaluate the snow depth estimation based on the equation derived from data in the remaining years (equation coefficients are shown in Table 2). The method proposed in Comiso et al. (2003) (hereafter called the Comiso method) was also applied for comparison. Data from 2016 were chosen randomly, and the large size of this dataset ensured that the evaluation was comprehensive. In addition, the OIB data in individual years were independent, which also ensured the evaluation's objectivity. The result showed that the proposed method obviously 220 outperformed the Comiso method with a mean difference of approximately -1.55 cm, while the latter had an average difference of -19.15 cm, which greatly underestimated the snow depth (Table 3).

Table 3. The comparisons between the OIB snow depth and the snow depth estimates from our method and Comiso' method in 2016. MD: mean difference, MAD: mean absolute difference.

	MD (cm)	MAD (cm)	RMSD (cm)	Correlation coefficient
Proposed method	-1.55	6.84	9.23	0.62
Comiso method	-19.15	19.15	21.26	0.60

225 In addition, the snow depth derived from the proposed method had a narrower numerical distribution when compared to the OIB data (Fig. 4a). A peak of 30 cm could be found in both the proposed method and the OIB snow depth distributions;



however, the Comiso method had a peak of 10 cm. This result confirms the conclusion of Worby et al. (2008a) that the Comiso method underestimates snow depth by a factor of 2. The snow depth estimated from the proposed method ranged from 20 to 60 cm, which was generally consistent with the OIB distribution. However, the OIB data had more snow depth values of < 20 cm (Fig. 4a). A quadratic fitting equation was assumed to improve this situation; however, the uncertainties of the derived equation coefficients were usually larger (Rostovsky et al., 2018).

Approximately 79% of the snow depth differences between the proposed method and OIB data had absolute differences of < 10 cm, while the Comiso method showed that only 15% of the absolute differences were less than 10 cm, and 80% of the absolute differences were greater than 10 cm (Fig. 4b). Although the snow depths estimated from the proposed method and the Comiso method had almost the same variation pattern as the OIB snow depth data (here, Eq. (1) was used), the Comiso method obviously underestimated the snow depth by a mean difference of -17.3 cm at the interannual scale, nearly equal to the minimum OIB snow depth (Fig. 4c). Hence, compared to OIB snow depth measurements, the proposed method not only had a closer snow depth distribution but also showed a consistent temporal variation pattern, which demonstrated its reliability for estimating Antarctic snow depth.

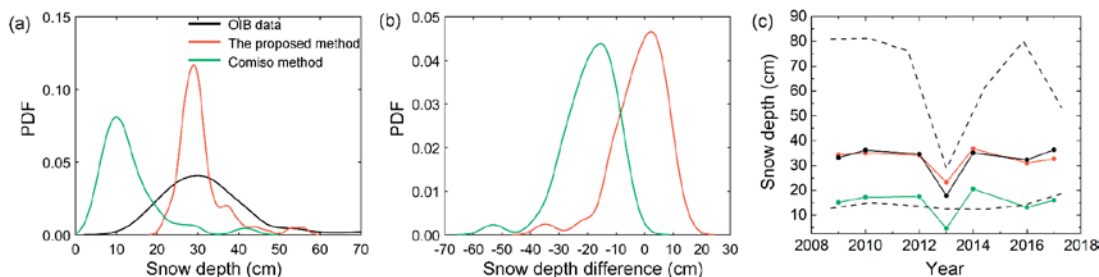


Figure 4. Comparisons of OIB snow depth to the snow depth estimates from both the proposed and Comiso method. (a) The distributions of snow depth estimates, (b) the probability density functions (PDFs) of differences between snow depth estimates and (c) the temporal variations of snow depth estimates. The black dashed lines in (c) show the variations in the maximum and minimum snow depth estimates from OIB.

4.2 Comparison to AADC in situ measurements in growth season

As mentioned previously, liquid water in the snow layer affects observed brightness temperatures and causes uncertainties in estimated snow depths. The proposed method was mainly used for snow depth derivation during the growing season. In this subsection, we focus on evaluating the performance of the proposed method during the growth season. AADC snow depth measurements were used for evaluation, and all AADC snow depth measurements within one microwave radiometer grid cell were averaged and compared to microwave radiometer-derived snow depth (from the proposed method and Comiso method, respectively). All AADC data used were collected during the growth season (i.e., November and December).



The result showed that the proposed method performed better than the Comiso method across all evaluation indices (Table 4) with a mean difference of 5.64 cm, which was clearly less than the 14.47 cm value obtained using the Comiso method. Although the number of AADC measurements were limited, the high accuracy and uneven distribution ensured the accuracy assessment was reliable and objective.

Table 4. The comparisons between the snow depth estimates from the proposed method and Comiso method and in situ measurements from AADC and ASPeCt. MD: mean difference, MAD: mean absolute difference.

	Comparison to AADC data		Comparison to ASPeCt data	
	Proposed method	Comiso method	Proposed method	Comiso method
MD (cm)	5.64	-14.47	8.62	-9.96
MAD (cm)	10.77	17.08	13.80	13.11
RMSD (cm)	13.79	19.49	16.85	17.61
Correlation coefficient	0.42	0.40	0.13	0.19
Number of grid cells	15	15	264	273

4.3 Comparison to ASPeCt shipboard observations in melting season

Although the AADC in situ data were more accurate, their amount was still limited. To evaluate the methods at larger spatial and temporal scales, ASPeCt shipboard observations were used for evaluation. More importantly, ASPeCt data include snow depth measurements during the melting season, which enabled us to test the applicability of the proposed method during this season. Overall, the proposed method performed slightly better than the Comiso method, which was clearly different when compared to AADC data (Table 4). ASPeCt snow depth data are usually obtained from thin ice regions, as ships tend to avoid thick ice; hence, the observed snow depth was with modal depths ranging between 0 and 10 cm (Worby et al., 2008b). In addition, the snow depth estimation equation from the Comiso method was derived from ASPeCt data, which might be unfair for the proposed method. Nevertheless, the proposed method still outperformed the Comiso method, and the similar performance demonstrated the reliability of the proposed method to estimate thin snow depth.

To show how the methods performed in different seasons and test the applicability of the proposed method during the melting season, in Fig. 5 we compared the microwave radiometer-derived snow depth to the ASPeCt snow depth observations during four seasons. The performances of the two methods during the four seasons were different. The proposed method was most accurate during autumn with an RMSD of 0.10 m (13 grid cells, the same hereinafter), followed by summer with an RMSD of 0.15 m (73), winter with an RMSD of 0.18 m (65) and spring with an RMSD of 0.18 m (113), which were nearly comparable. For the Comiso method, accuracy was highest during winter with an RMSD of 0.10 m (65), followed by autumn with an RMSD of 0.14 m (11), summer with an RMSD of 0.15 m (77) and spring with an RMSD of 0.22 m (119). A larger bias was found in spring than in other seasons. Overall, the proposed method was better than or



280 comparable to the Comiso method during spring, summer and autumn. However, it should be noted that, the amount of data may also affect the performance comparison.

Tables 5 and 6 show the seasonal evaluation of the mentioned two methods in Antarctic six sea sectors (Weddell West: 300°–315°, Weddell East: 315°–20°, Indian Ocean: 20°–90°, Pacific Ocean: 90°–160°, Ross Sea: 160°–230°, Bellingshausen-Amundsen Sea: 230°–300°). It should be noted that in some sea sectors, we could not construct the evaluations during all four seasons, due to the limited distribution of ASPeCt data. Both methods have lower accuracies in the Weddell West sector, which may be due to the thicker snow there, as most of the multiyear ice is in the Weddell West. Comparatively, the Comiso method underestimated snow depth in all sea sectors and seasons. Due to the accuracy of ASPeCt samples, the evaluation may be biased, but ASPeCt shipborne data still provide a proxy for performance evaluation. More importantly, no obvious differences could be found during different seasons in individual sea sectors, and the proposed method achieved a comparable or better performance in summer than in other seasons. Hence, the proposed method can still estimate snow depth during the melting season.

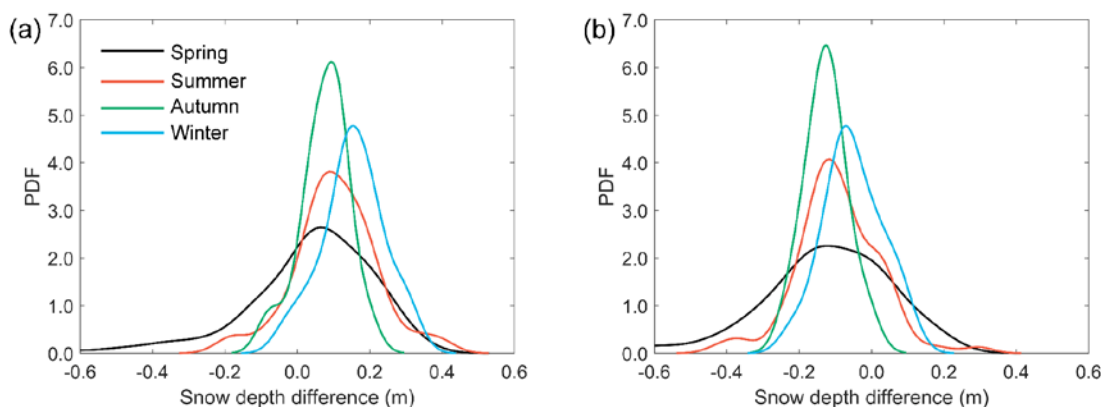


Figure 5. The probability density functions (PDFs) of snow depth estimates differences of the proposed method (a) and Comiso method (b) by comparing to ASPeCt shipborne data in four seasons.

295

Table 5. The comparisons between the snow depth estimates from proposed method and in situ measurements from ASPeCt in different sea sectors and seasons. MD: mean difference, MAD: mean absolute difference.

	Season	MD (cm)	MAD (cm)	RMSD (cm)	Correlation coefficient	Number of grid cells
Weddell West	Spring	-0.07	-0.13	0.19	0.30	21
	Summer	0.15	0.19	0.23	-0.03	10
Weddell East	Spring	0.13	0.17	0.19	-0.37	48
	Summer	-0.10	0.10	0.10	1	1
	Winter	0.14	0.14	0.14	-0.39	16
Indian Ocean	Spring	0.12	0.12	0.12	0.49	3
Pacific Ocean	Spring	-0.05	0.15	0.20	-0.16	26
	Autumn	-0.08	0.08	0.08	1	1
	Winter	0.13	0.14	0.14	0.14	10



Ross Sea	Spring	0.02	0.05	0.06	0.31	15
	Summer	0.10	0.12	0.14	0.07	62
	Autumn	0.09	0.09	0.10	0.43	12
Bellingshausen-Amundsen Sea	Winter	0.17	0.17	0.19	0.20	39

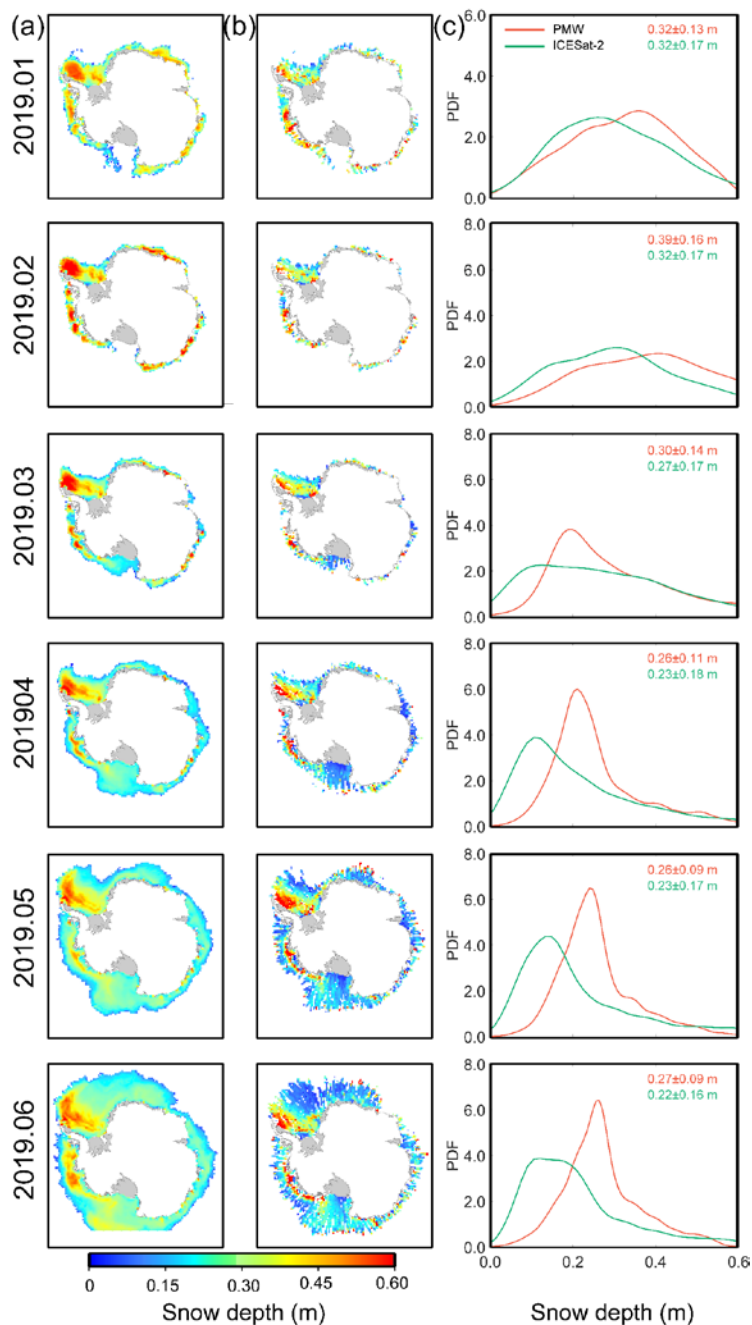
300 Table 6. The comparisons between the snow depth estimates from Comiso method and in situ measurements from ASPeCt in different sea sectors and seasons. MD: mean difference, MAD: mean absolute difference.

	Season	MD (cm)	MAD (cm)	RMSD (cm)	Correlation coefficient	Number of grid cells
Weddell West	Spring	-0.24	0.24	0.29	0.34	22
	Summer	-0.06	0.15	0.18	0.45	11
Weddell East	Spring	-0.02	0.11	0.15	-0.31	49
	Summer	-0.16	0.16	0.17	1	2
	Winter	-0.08	0.08	0.09	-0.50	16
Indian Ocean	Spring	-0.03	0.05	0.07	0.85	4
Pacific Ocean	Spring	-0.27	0.27	0.33	-0.16	24
	Winter	-0.08	0.08	0.10	0.34	10
Ross Sea	Spring	-0.12	0.13	0.15	0.28	20
	Summer	-0.10	0.11	0.14	0.03	65
	Autumn	-0.13	0.13	0.14	0.14	11
Bellingshausen-Amundsen Sea	Winter	-0.03	0.08	0.10	0.24	39

4.4 Comparison to satellite laser altimeter-derived snow depth data in both spatial and temporal scales

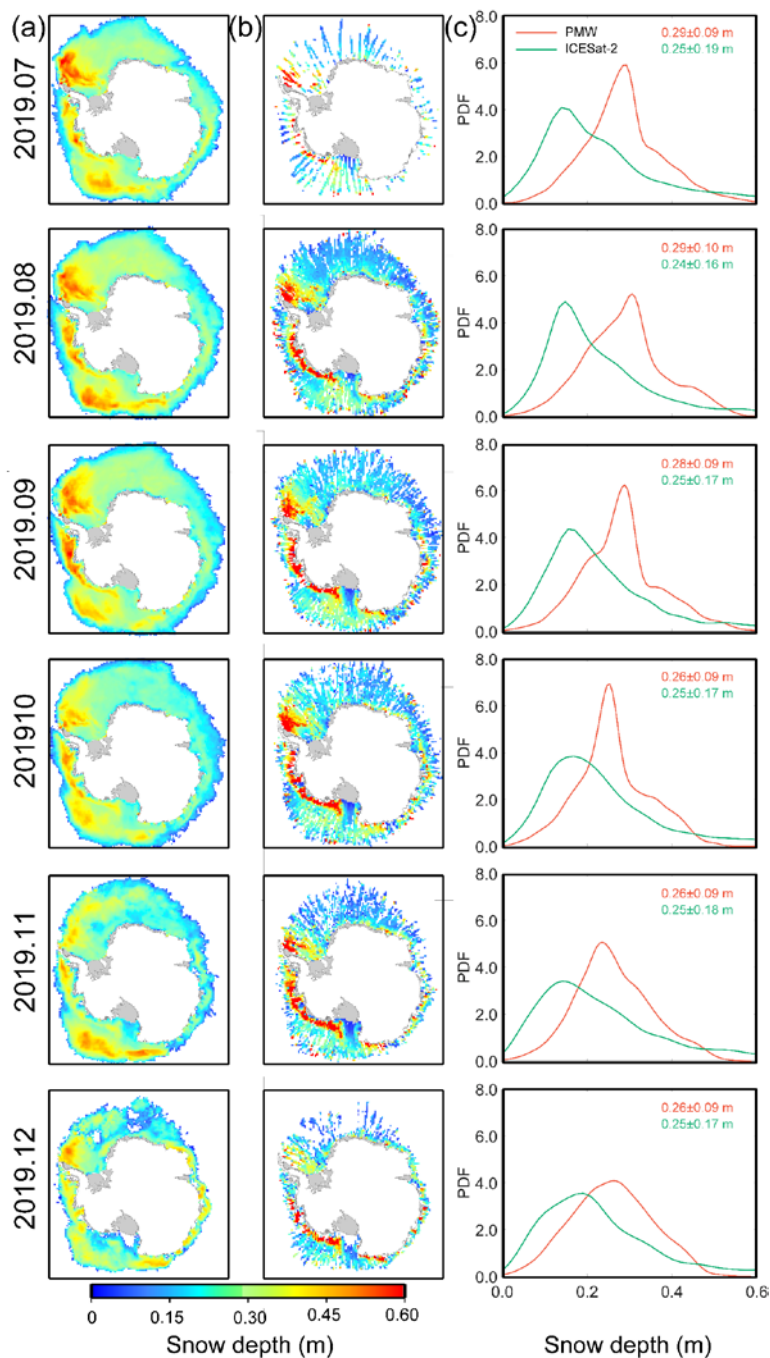
Kern et al. (2016) found that satellite laser altimeters can be used to estimate snow depth over Antarctic sea ice with a low level of uncertainty, and these snow depth measurements agreed closely with both shipborne and airborne data. Considering the potential reliability of satellite laser altimeter-derived snow depth, following Kern et al. (2016), we estimated the Antarctic snow depth in a complete year (January 2019 to December 2019) from ICESat-2 using a linear equation based on total freeboard and compared the results to estimates from the proposed method, as shown in Figs. 6 and 7. Generally, the snow depths estimated by the proposed method agreed closely with those derived from laser altimeters. Both snow depth datasets showed deeper snow cover mainly in the Weddell West and Bellingshausen-Amundsen Sea sectors.

310 As satellite laser altimetry is independent of the snow properties, satellite laser altimeters can better reveal snow depth evolution. Fig. 8 shows the monthly snow depth evolution in 2019 based on the two methods. Overall, the two snow depth times were highly consistent and have an RMSD of 3 cm and a correlation coefficient of 0.86. Although the snow depth ranges from the two datasets still have some differences, the overall variation patterns were similar. The existing differences in snow depth range and variation pattern were due to sensor and method differences. High consistency between the two datasets on both spatial and temporal scales implies the reliability of the proposed method.



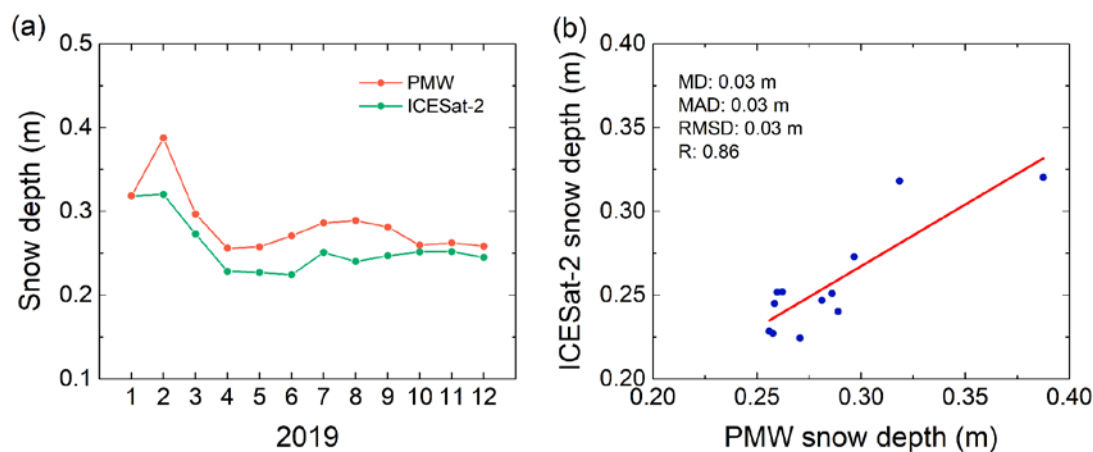
315

Figure 6. The spatial distributions and probability density functions (PDFs) of snow depth based on the proposed method and ICESat-2 between January and June 2019. The averaged snow depth value and its standard deviation value are shown in the upper right corner of (c), red for snow depth estimated from the proposed method, i.e., based on passive microwave radiometer (PMW), green for ICESat-2 snow depth.



320

Figure 7. The spatial distributions and probability density functions (PDFs) of snow depth based on the proposed method and ICESat-2 between July and December 2019. The averaged snow depth value and its standard deviation value are shown in the upper right corner of (c), red for snow depth estimated from the proposed method, i.e., based on passive microwave radiometer (PMW), green for ICESat-2 snow depth.



325

Figure 8. (a) Time series of the snow depth based on the proposed method (red), i.e., based on a passive microwave radiometer (PMW) and ICESat-2 (green) between January and December 2019. (b) Scatter diagrams of snow depth estimated from the proposed method and ICESat-2. The evaluation indices are also shown in (b); MD: mean difference, MAD: mean absolute difference, R: correlation coefficient.

330 5 Spatio-temporal variation of Antarctic snow depth from 2002 to 2020

Although the proposed method was initially applied for snow depth estimation during the growing season, comparable performances were still found during the melting season; hence, we estimated the snow depth for all seasons from 2002 to 2020 and analysed the spatiotemporal variation pattern. The averaged Antarctic snow depth distributions from 2002 to 2020 showed obvious seasonal patterns (Fig. 9). In all four seasons, thin snow covers were seen in the marginal sea ice and thicker snow was located in the Weddell West and Bellingshausen/Amundsen Sea sectors, which was more obvious in summer. In winter, sea ice expands, and thicker snow cover could be found.

Antarctic snow depth showed significant decreasing trends of -0.13 cm/yr from 2002 to 2020 (Table. 7). This snow depth trend of Antarctic sea ice is the combined result from the six sea sectors, and the trend of snow depth may be "enhanced" or "offset". Hence, it is necessary to analyse the trend for individual sea sectors. All six sea sectors showed decreasing trends, and these trends were decreasing across all four seasons.

340

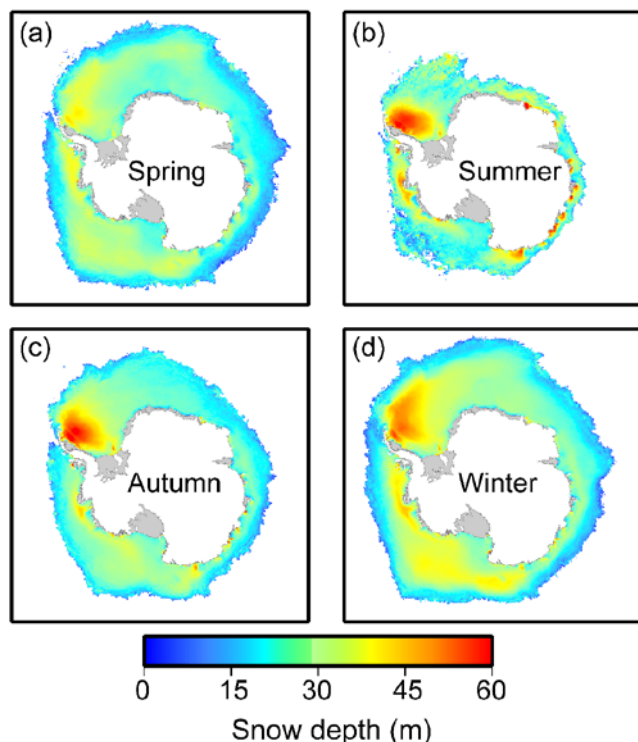


Figure 9. The spatial distributions of averaged snow depth in different seasons from 2002 to 2020.

Table 7. The interannual and seasonal trends of snow depth estimates in Antarctica and six sea sectors from 2002 to 2020.

	Year (cm/yr)	Spring (cm/season)	Summer (cm/season)	Autumn (cm/season)	Winter (cm/season)
Antarctica	-0.13*	-0.15*	-0.14	-0.17**	-0.11*
Weddell West	-0.02	-0.07	-0.06	-0.08	-0.02
Weddell East	-0.20*	-0.22**	-0.39*	-0.15*	-0.04
Indian Ocean	-0.12	-0.10	-0.12	-0.14*	-0.10*
Pacific Ocean	-0.14*	-0.05	-0.29**	-0.15	-0.11
Ross Sea	-0.27**	-0.27*	-0.41*	-0.33*	-0.14
Bellingshausen- Amundsen Sea	-0.17	-0.10	-0.14	-0.28	-0.24*

345 * and ** means that the trend is significant at 95% and 99% significance level according to two-tailed Student's t-tests, respectively.

The spatial distributions of snow depth variation trends during four seasons from 2002 to 2020 are shown in Fig. 10. During spring, except for the marginal sea ice in West Antarctica, the snow depth in other regions showed clear decreasing
 350 trends. During summer and autumn, negative trends could be found in the Weddell West sector. During winter, a positive trend was found in the marginal sea ice of the Weddell West sector and West Ross Sea, while a decreasing trend was found in other sea sectors. In general, decreasing trends dominated the snow cover over Antarctic sea ice.

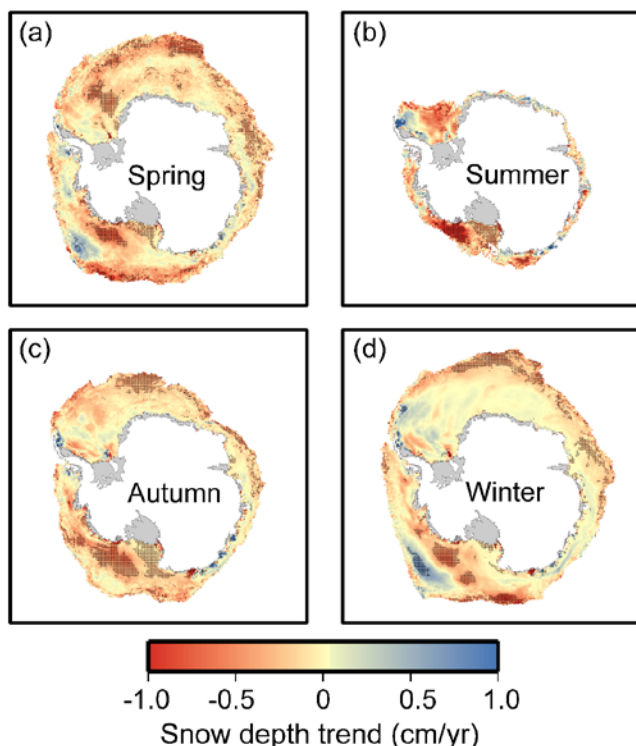


Figure 10. The spatial distributions of snow depth trends in different seasons from 2002 to 2020. The black dot means that
355 the trend is significant at 95% significance level according to two-tailed Student's t-tests.

6 Discussions

6.1 The uncertainty from estimation method

Growth and melting of the snow layer will change the observed brightness temperatures; hence, the numerical relationship
360 between brightness temperatures and snow depth is not fixed. When the snow layer starts to melt, its emissivity greatly
differs from that of dry snow, which causes some biases in the snow depth estimation (Willmes et al., 2014). In the present
study, we still estimated the snow depth during the melting season with the following assumptions: 1) surface melting in
Antarctica is not as strong as that in the Arctic, and 2) the evaluation shows the performance of the proposed method is
comparable during the growth and melting seasons. The latter may be due to the application of lower frequencies, as they
365 suffer less from the volume scattering caused by the seasonal variation in the snow layer (such as densification or grain size
increase, Rostosky et al., 2018). However, because lower frequencies are less sensitive to thin snow there may be some
biases for snow depth in early winter. This result explains why the proposed method performed slightly better than the
Comiso method when compared with thinner ASPeCt snow depth. Since the snow depth over Antarctic sea ice is thicker



than that in the Arctic and lower frequencies are more sensitive to thicker snow (Rostosky et al., 2018), this influence is
370 assumed to be limited.

In addition, at the end of winter or early spring, the top snow layer melts during the day and refreezes at night. This forms
an ice layer in the snow. This ice layer will enhance the scattering intensity and lead to overestimated snow depth. In
Antarctica, the ice-covered snow layer may be covered by new snow (Willatt et al., 2009) and this melt–refreeze cycle will
result in further overestimation. In addition, the relationship between brightness temperatures and snow depth is affected by
375 snow density, snow grain size, flooded sea ice and weather conditions. However, because in situ measurements of these
snow and ice properties are infrequently collected, their influences cannot be quantified and are thus not considered in the
existing method. This issue can be solved with future in situ measurements. Lower frequencies are less affected by these
factors and are more sensitive to deeper snow. Thus, they can improve the current Antarctic snow depth estimation. However,
they are also more sensitive to roughness on the sea ice surface (Stroeve et al., 2006), and the spatial differences in snow
380 emissivity derived from snow metamorphism in Antarctica are rather small (Willmes et al., 2014). Nevertheless, similar
performances of estimated snow depth with those derived from ICESat-2 at both spatial and temporal scales still demonstrate
the reliability of the proposed method and imply that the snow depth uncertainties caused by the factors mentioned above are
relatively small and acceptable, as satellite laser altimeters are independent of snow properties.

Although the inclusion of low frequencies can reduce these influences, the linear regression equation may be too simple
385 for some situations, e.g., very thin or thick snow. Some complex methods, e.g., polynomial fitting equations (Kilic et al.,
2019), random forest regression models (Winstrup et al., 2019) and neural network models (Braakmann-Folgmann et al.,
2019), may improve these situations. However, all these methods require more snow depth samples and much more training
data if complex machine learning or deep learning technologies are used. Antarctic samples are quite sparse. Considering
these potential limitations and the lack of a better operational snow depth product, we assume that the linear equation can
390 estimate Antarctic snow depth more robustly in the current stage.

6.2 The uncertainty from OIB data

Since the derivation of the regression coefficients in Eq. (1) and Eq. (2) directly depends on the applied OIB samples, the
uncertainty from the OIB data has a direct influence on snow depth estimation. Most of the OIB airborne measurements were
taken in West Antarctica during October or November, and their spatiotemporal representativeness was hence limited.
395 Nevertheless, it was the most suitable data source for equation derivation considering its large spatial and temporal scales.
The comparisons to ASPeCt and AADC data both demonstrated that this equation could be used in all seasons and sea
sectors. Limited by the extreme climate and oceanic conditions in Antarctica, in situ Antarctic sea ice measurement data are
still limited. When more in situ data can be obtained, the corresponding algorithm can be further improved.



6.3 The uncertainty from sea ice types

400 It is still difficult for microwave radiometers to estimate snow depth over multiyear ice because multiyear ice scattering
properties are similar to snow. On the one hand, reliable sea ice type data in Antarctica was not accessible until now, and we
still cannot derive snow depth estimation equations for different ice types. On the other hand, Antarctic sea ice is mostly
young, first year ice. Multiyear ice is mainly located in the Weddell West sector. No obvious overestimations could be found
when comparing the ASPeCt data in the Weddell West sector to data from both methods (as shown in Tables 5 and 6). In
405 most cases, thickness was underestimated, which indicated that the underlying ice did not affect the radiometer signals.
Hence, the influence of multiyear ice on snow depth estimation was assumed to be limited, and bias was mostly introduced
by snow properties. This will be further improved when accurate Antarctic sea ice type data and in situ measurements are
available.

6.4 The uncertainty from applied spatial resolution

410 Coarser spatial resolutions cannot obtain a detailed spatial pattern of snow depth. Although optical or SAR images have fine
spatial resolutions, they still cannot estimate Antarctic snow depth on a daily scale. The microwave radiometer is one of the
most effective sensors for daily Antarctic snow depth derivation. Although the current spatial resolution of the microwave
radiometer is relatively coarse (25–50 km), considering the relatively flat surface of Antarctic sea ice and the urgent need for
snow depth over Antarctic sea ice, the uncertainty caused by the coarser resolution is acceptable.

415 7 Data availability

Snow depth product (including snow depth uncertainty) over Antarctic sea ice can be downloaded from National Tibetan
Plateau Data Center, Institute of Tibetan Plateau Research, Chinese Academy of Sciences at
<http://data.tpdc.ac.cn/en/disallow/61ea8177-7177-4507-aeeb-0c7b653d6fc3/> (Shen and Ke, 2021, DOI:
10.11888/Snow.tpdc.271653). A short summary and some auxiliary information (including file naming, required software
420 and etc.) are also provided.

8 Conclusions

Our study updates the regression equation for estimating snow depth over Antarctic sea ice using microwave radiometers. By
comparing 7-year OIB snow depth measurements, we found that the GR calculated from both lower and higher frequencies,
i.e., GR(37/7), was best for deriving the Antarctic snow depth. It had an RMSD is 8.92 cm and a correlation coefficient of -
425 0.64. The derived equation based on GR(37/7) was applied at consistent brightness temperatures from AMSR-E and AMSR-
2. To fill the observation gaps between AMSR-E and AMSR-2, we used SSMIS data with a new equation based on
GR(37/19) with a correction applied for consistent snow depth estimation. The estimated snow depth uncertainty analysis



used a Gaussian error propagation. The mean uncertainty of the micrometer radiometer-derived snow depth was 3.81 cm, with an average ratio of 12%, dependent on snow depth.

430 The self-evaluation based on the combination of OIB data in different years showed no obvious interannual variations could be found in the regression coefficients. The uncertainty of slopes from different combinations of OIB data was 42.85, which resulted in a snow depth estimation bias of <1 cm. The proposed method agreed well with the OIB data, showing a mean difference of -1.55 cm, and there was a similar snow depth variation pattern at the interannual scale. The Comiso method underestimated snow depth, with an average difference of -19.15 cm.

435 AADC data provided a comprehensive and unbiased assessment because they include measurements of both thick and thin snow layers. In comparison to AADC in situ measurements, the proposed method outperformed the Comiso method, with a smaller mean difference of 5.64 cm and an RMSD of 13.79 cm. The Comiso method underestimated snow depth with a mean difference of -14.47 cm and an RMSD of 19.49 cm.

We suggest the proposed method be used during the growth season; however, the comparison to ASPeCt shipborne
440 observations implied that this method could also be used during the melting season. The comparison showed that the proposed method had slightly better performance than the Comiso method (RMSDs of 16.85 cm and 17.61 cm, respectively) because the ASPeCt shipborne observations were focused on thin ice. The evaluation may be somewhat biased due to the observational accuracy of ASPeCt data (a mean bias of 20% or 30%). Nevertheless, comparable accuracies could be found during both the growth and the melting seasons, suggesting that the proposed method could be applied in all seasons.

445 Although the proposed method had better performance, it could still be improved. Because a sufficient operational snow depth product is still lacking, we used our proposed method to generate a new, updated time series product of snow depth over Antarctic sea ice from 2002 to 2020 (including melting season) on a daily scale. A decreasing trend of snow depth could be found in all six sectors and four seasons at the interannual scale. In addition, this dataset can be used to re-analyse data and acts as an input for sea ice thickness estimation.

450

Author contribution

Xiaoyi Shen and Haili Li developed the related algorithm, generated and evaluated the snow depth product; Chang-Qing Ke supervised this work.

Competing interests

455 The authors declare that they have no conflict of interest.

Disclaimer

Publisher's note: Copernicus Publications remains neutral with regard to jurisdictional claims in published maps and institutional affiliations.



Special issue statement

460 This article is part of the special issue “Extreme environment datasets for the three poles”. It is not associated with a conference.

Acknowledgments

465 AMSR-E brightness temperature data are derived at https://nsidc.org/data/AE_SI25/versions/3; AMSR-2 brightness temperature data can be derived at https://nsidc.org/data/AU_SI25/versions/1; SSMIS brightness temperature data are derived at <https://nsidc.org/data/NSIDC-0001/versions/4>; OIB airborne data can be derived at <https://nsidc.org/data/ILATM2/versions/2>; ASPeCt Data are derived at <http://aspect.antarctica.gov.au/data>; AADC in situ data can be derived at <https://nsidc.org/data/G10011/versions/2>. We thank all the data providers for their data.

Financial support

470 This work is supported by the Programs for National Natural Science Foundation of China [grant numbers 41976212, 41830105].

References

- Braakmann-Folgmann, A. and Donlon, C.: Estimating snow depth on Arctic sea ice using satellite microwave radiometry and a neural network, *The Cryosphere*, 13, 2421-2438, <https://doi.org/10.1029/AR074p0019>, 2019.
- 475 Cavalieri, D. J., Gloersen, P., and Campbell, W. J.: Determination of sea ice parameters with the Nimbus 7 SMMR, *J. Geophys. Res.-Atmos.*, 89, 5355-5369, <https://doi.org/10.1029/JD089iD04p05355>, 1984.
- Comiso, J. C., Cavalieri, D. J., and Markus, T.: Sea ice concentration, ice temperature, and snow depth using AMSR-E data, *IEEE Trans. Geosci. Remote Sens.*, 41, 243-252, <https://doi.org/10.1109/TGRS.2002.808317>, 2003.
- Du, J., Kimball, J. S., Shi, J., Jones, L. A., Wu, S., Sun, R., and Yang, H.: Inter-calibration of satellite passive microwave land observations from AMSR-E and AMSR2 using overlapping FY3B-MWRI sensor measurements, *Remote Sens.*, 6, 8594-8616, <https://doi.org/10.3390/rs6098594>, 2014.
- 480 Giles, K. A., Laxon, S. W., and Worby, A. P.: Antarctic sea ice elevation from satellite radar altimetry, *Geophys. Res. Lett.*, 35, <https://doi.org/10.1029/2007GL031572>, 2008.
- Kern, S. and Ozsoy-Çiçek, B.: Satellite remote sensing of snow depth on Antarctic Sea Ice: An inter-comparison of two empirical approaches, *Remote Sens.*, 8, 450, <https://doi.org/10.3390/rs8060450>, 2016.
- 485 Kern, S. and Spreen, G.: Uncertainties in Antarctic sea-ice thickness retrieval from ICESat, *Ann. Glaciol.*, 56, 107-119, <https://doi.org/10.3189/2015AoG69A736>, 2015.



- Kern, S., Ozsoy-Cicek, B., Willmes, S., Nicolaus, M., Haas, C., and Ackley, S.: An intercomparison between AMSR-E snow-depth and satellite C-and Ku-band radar backscatter data for Antarctic sea ice, *Ann. Glaciol.*, 52, 279-290, 490 <https://doi.org/10.3189/172756411795931750>, 2011.
- Kilic, L., Tonboe, R. T., Prigent, C., and Heygster, G.: Estimating the snow depth, the snow–ice interface temperature, and the effective temperature of Arctic sea ice using Advanced Microwave Scanning Radiometer 2 and ice mass balance buoy data, *The Cryosphere*, 13, 1283-1296, <https://doi.org/10.5194/tc-13-1283-2019>, 2019.
- Krabill, W., Thomas, R., Martin, C., Swift, R., and Frederick, E.: Accuracy of airborne laser altimetry over the Greenland ice 495 sheet, *Int. J. Remote Sens.*, 16, 1211-1222, <https://doi.org/10.1080/01431169508954472>, 1995.
- Kurtz, N., Farrell, S., Studinger, M., Galin, N., Harbeck, J., Lindsay, R., Onana, V., Panzer, B., and Sonntag, J.: Sea ice thickness, freeboard, and snow depth products from Operation IceBridge airborne data, *The Cryosphere*, 7, 1035-1056, <https://doi.org/10.5194/tc-7-1035-2013>, 2013.
- Kwok, R. and Maksym, T.: Snow depth of the Weddell and Bellingshausen sea ice covers from ice bridge surveys in 2010 500 and 2011: An examination, *J. Geophys. Res.-Oceans*, 119, 4141-4167, <https://doi.org/10.1002/2014JC009943>, 2014.
- Kwok, R. and Untersteiner, N.: The thinning of Arctic sea ice, *Phys. Today*, 64, 36-41, 2011.
- Kwok, R., Kacimi, S., Webster, M., Kurtz, N., and Petty, A.: Arctic snow depth and sea ice thickness from ICESat-2 and CryoSat-2 freeboards: a first examination, *J. Geophys. Res.-Oceans*, 125, e2019JC016008, <https://doi.org/10.1029/2019JC016008>, 2020.
- 505 Li, H., Xie, H., Kern, S., Wan, W., Ozsoy, B., Ackley, S., and Hong, Y.: Spatio-temporal variability of Antarctic sea-ice thickness and volume obtained from ICESat data using an innovative algorithm, *Remote Sens. Environ.*, 219, 44-61, <https://doi.org/10.1016/j.rse.2018.09.031>, 2018.
- Maaß, N., Kaleschke, L., Tian-Kunze, X., and Drusch, M.: Snow thickness retrieval over thick Arctic sea ice using SMOS satellite data, *The Cryosphere*, 7, 1971-1989, <https://doi.org/10.5194/tc-7-1971-2013>, 2013.
- 510 Markus, T. and Cavalieri, D. J.: Snow depth distribution over sea ice in the Southern Ocean from satellite passive microwave data, *Antarctic sea ice: physical processes, interactions and variability*, 74, 19-39, <https://doi.org/10.1029/AR074p0019>, 1998.
- Markus, T., Powell, D. C., and Wang, J. R.: Sensitivity of passive microwave snow depth retrievals to weather effects and snow evolution, *IEEE T. Geosci. Remote Sens.*, 44, 68-77, <https://doi.org/10.1109/TGRS.2005.860208>, 2005.
- Martin, C. F., Krabill, W. B., Manizade, S., Russell, R., Sonntag, J. G., Swift, R. N., and Yungel, J. K.: Airborne 515 Topographic Mapper Calibration Procedures and Accuracy Assessment, NASA Technical Reports, Vol. 20120008479(NASA/TM-2012-215891, GSFC.TM.5893.2012), <http://hdl.handle.net/2060/20120008479>, 32 pp., Natl. Aeronaut. and Space Admin., Washington, D. C, 2012.
- Massom, R. A., Eicken, H., Hass, C., Jeffries, M. O., Drinkwater, M. R., Sturm, M., Worby, A. P., Wu, X., Lytle, V. I., and Ushio, S.: Snow on Antarctic sea ice, *Reviews Geophysics*, 39, 413-445, <https://doi.org/10.1029/2000RG000085>, 2001.
- 520 Maykut, G. A. and Untersteiner, N.: Some results from a time-dependent thermodynamic model of sea ice, *J. Geophys. Res.*, 76, 1550-1575, <https://doi.org/10.1029/JC076i006p01550>, 1971.



- Ozsoy-Cicek, B., Ackley, S., Xie, H., Yi, D., and Zwally, J.: Sea ice thickness retrieval algorithms based on in situ surface elevation and thickness values for application to altimetry, *J. Geophys. Res.-Oceans*, 118, 3807-3822, <https://doi.org/10.1002/jgrc.20252>, 2013.
- 525 Petrich, C., Eicken, H., Polashenski, C. M., Sturm, M., Harbeck, J. P., Perovich, D. K., and Finnegan, D. C.: Snow dunes: A controlling factor of melt pond distribution on Arctic sea ice, *J. Geophys. Res.-Oceans*, 117, <https://doi.org/10.1029/2012JC008192>, 2012.
- Rostosky, P., Spreen, G., Farrell, S. L., Frost, T., Heygster, G., and Melsheimer, C.: Snow depth retrieval on Arctic sea ice from passive microwave radiometers—Improvements and extensions to multiyear ice using lower frequencies, *J. Geophys. Res.-Oceans*, 123, 7120-7138, <https://doi.org/10.1029/2018JC014028>, 2018.
- 530 Schenk, T., Csatho, B., and Lee, D.: Quality control issues of airborne laser ranging data and accuracy study in an urban area, *Int. Arch. Photogramm. Remote Sens.*, 32, 101-108, 1999.
- Spreen, G., Kaleschke, L., and Heygster, G.: Sea ice remote sensing using AMSR-E 89-GHz channels, *J. Geophys. Res.-Oceans*, 113, <https://doi.org/10.1029/2005JC003384>, 2008.
- 535 Shen, X., and Ke, C-Q.: Snow depth product over Antarctic sea ice from 2002 to 2020, National Tibetan Plateau Data Center [data set], <http://data.tpdac.cn/en/disallow/61ea8177-7177-4507-aeeb-0c7b653d6fc3/>, 2021.
- Stroeve, J. C., Markus, T., Maslanik, J. A., Cavalieri, D. J., Gasiewski, A. J., Heinrichs, J. F., Holmgren, J., Perovich, D. K., and Sturm, M.: Impact of surface roughness on AMSR-E sea ice products, *IEEE T. Geosci. Remote Sens.*, 44, 3103-3117, <https://doi.org/10.1109/TGRS.2006.880619>, 2006.
- 540 Sturm, M., Perovich, D. K., and Holmgren, J.: Thermal conductivity and heat transfer through the snow on the ice of the Beaufort Sea, *J. Geophys. Res.-Oceans*, 107, SHE 19-11-SHE 19-17, <https://doi.org/10.1029/2000JC000409>, 2002.
- Webster, M., Gerland, S., Holland, M., Hunke, E., Kwok, R., Lecomte, O., Massom, R., Perovich, D., and Sturm, M.: Snow in the changing sea-ice systems, *Nature Climate Change*, 8, 946-953, <https://doi.org/10.1038/s41558-018-0286-7>, 2018.
- Willatt, R. C., Giles, K. A., Laxon, S. W., Stone-Drake, L., and Worby, A. P.: Field investigations of Ku-band radar penetration into snow cover on Antarctic sea ice, *IEEE T. Geosci. Remote Sens.*, 48, 365-372, <https://doi.org/10.1109/TGRS.2009.2028237>, 2009.
- 545 Willmes, S., Nicolaus, M., and Haas, C.: The microwave emissivity variability of snow covered first-year sea ice from late winter to early summer: a model study, *The Cryosphere*, 8, 891-904, <https://doi.org/10.5194/tc-8-891-2014>, 2014.
- Winstrup, M., Tonboe, R., Lavergne, T., Rasmussen, T., Saldo, R., Tietsche, S., and Pedersen, L. T.: Retrieval of spring-time snow thicknesses on Arctic sea ice from AMSR-2 microwave radiometer data, eSA Living Planet Symposium 2019, Milan, Italy, 13–17 May 2019.
- 550 Worby, A. P., Markus, T., Steer, A. D., Lytle, V. I., and Massom, R. A.: Evaluation of AMSR-E snow depth product over East Antarctic sea ice using in situ measurements and aerial photography, *J. Geophys. Res.-Oceans*, 113, <https://doi.org/10.1029/2007JC004181>, 2008a.



- 555 Worby, A. P., Geiger, C. A., Paget, M. J., Van Woert, M. L., Ackley, S. F., and DeLiberty, T. L.: Thickness distribution of Antarctic sea ice, *J. Geophys. Res.-Oceans*, 113, <https://doi.org/10.1029/2007JC004254>, 2008b.
- Xie, H., Tekeli, A. E., Ackley, S. F., Yi, D., and Zwally, H. J.: Sea ice thickness estimations from ICESat Altimetry over the Bellingshausen and Amundsen Seas, 2003–2009, *J. Geophys. Res.-Oceans*, 118, 2438-2453, <https://doi.org/10.1002/jgrc.20179>, 2013.
- 560 Zwally, H. J., Yi, D., Kwok, R., and Zhao, Y.: ICESat measurements of sea ice freeboard and estimates of sea ice thickness in the Weddell Sea, *J. Geophys. Res.-Oceans*, 113, <https://doi.org/10.1029/2007JC004284>, 2008.
- Zwally, H. J., Comiso, J. C., Parkinson, C. L., Cavalieri, D. J., and Gloersen, P.: Variability of Antarctic sea ice 1979–1998, *J. Geophys. Res.-Oceans*, 107, 9-1-9-19, <https://doi.org/10.1029/2000JC000733>, 2002.